analytical chemistry

pubs.acs.org/ac Article

Integrated Microfluidic Chip for Rapid Antimicrobial Susceptibility Testing Directly from Positive Blood Cultures

Meijia Zhu, Teng Xu, Yongqiang Cheng,* Bo Ma, Jian Xu, Zhidian Diao, Fei Wu, Jing Dai, Xiao Han, Pengfei Zhu, Chao Pang, Jing Li, Hongwei Wang, Ranran Xu, and Xiaotong Li

Cite This: *Anal. Chem.* 2023, 95, 14375−14383 Read Online

ACCESS | Metrics & More | Article Recommendations | Supporting Information

ABSTRACT: Rapid and accurate antimicrobial prescriptions are critical for bloodstream infection (BSI) patients, as they can guide drug use and decrease mortality significantly. The traditional antimicrobial susceptibility testing (AST) for BSI is time-consuming and tedious, taking 2−3 days. Avoiding lengthy monoclonal cultures and shortening the drug sensitivity incubation time are keys to accelerating the AST. Here, we introduced a bacteria separation integrated AST (BSI-AST) chip, which could extract bacteria directly from positive blood cultures (PBCs) within 10 min and quickly give susceptibility information within 3 h. The integrated chip includes a bacteria separation chamber, multiple AST chambers, and connection channels. The separator gel was first preloaded into the bacteria separation chamber, enabling the swift separation of bacteria cells from PBCs through on-chip centrifugation. Then, the bacteria suspension was distributed in the AST chambers with preloaded antibiotics through a quick vacuum-assisted aliquoting strategy. Through centrifuge-assisted on-chip enrichment, detectable growth of the phenotype under different antibiotics could be easily observed in the taper tips of AST chambers within a few hours. As a proof of concept, direct AST from artificial PBCs with *Escherichia coli* against 18 antibiotics was performed on the BSI-AST chip, and the whole process from bacteria extraction to AST result output was less than 3.5 h. Moreover, the integrated chip was successfully applied to the diagnosis of clinical PBCs, showing 93.3% categorical agreement with clinical standard methods. The reliable and fast pathogen characterization of the integrated chip suggested its great potential application in clinical diagnosis.

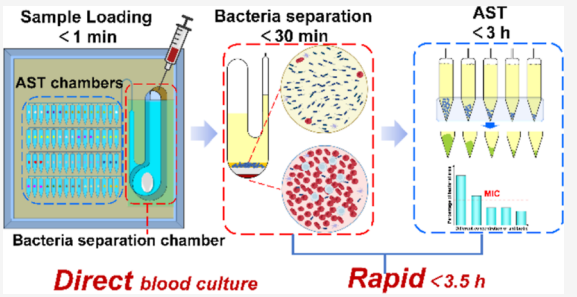

INTRODUCTION

Bloodstream infection (BSI) is a type of infectious disease caused by the invasion of pathogenic microorganisms into the bloodstream. In some cases, BSI can develop into sepsis, which is one of the critical diseases in the ICU.[1] According to a 6 year long retrospective study conducted in the US, the incidence of BSI in hospitalized patients was 5.9%, and the case-fatality rate was 15.6%.[2] Moreover, about 40% of patients with sepsis or sepsis shock are caused by BSIs.[3] Shockingly, sepsis affects 47 to 50 million people, and at least 11 million die every year worldwide. The main reason for the high morbidity and mortality rates lies in the inability to give effective antibiotic treatment early in the disease onset. Unfortunately, the empirical broad-spectrum antimicrobial therapy currently used in hospitals not only facilitates the selection and spread of drug-resistant pathogens but also increases the risk of fungal infections.[4,5] In an era of global antibiotic resistance and the absence of new antimicrobial drug development,[6−8] there is a pressing need for rapid diagnosis and antimicrobial susceptibility testing (AST) of BSIs, which is a prerequisite for timely targeted antibiotic therapy and particularly important for improving the survival and prognosis of patients.[9]

For the low concentrations of infecting bacteria in blood, about 1−100 colony-forming-units (CFU) per mL, which is 10^7 to 10^9 times lower than that of mammalian blood cells, blood culturing is still the gold standard for BSI diagnosis.[10] The traditional AST methods widely used in clinical microbiology laboratories, including broth microdilution, disk diffusion, E-test, and automated systems, still rely heavily on further overnight subcultures after blood cultures, which are laborious and time-consuming.[11−13] The whole procedure often lasts over 3 days because of the three overnight culture steps involved: blood culture, subculture, and AST culture.[14] Therefore, avoiding lengthy monoclonal cultures and shortening the incubation of drug sensitivity are the keys to accelerating the AST of BSIs.

Recently, microfluidic methods have been utilized for bacterial analysis owing to their speed, high throughput, and

Received: June 23, 2023
Accepted: September 5, 2023
Published: September 15, 2023

https://doi.org/10.1021/acs.analchem.3c02737
Anal. Chem. 2023, 95, 14375−14383

small footprint. Various microfluidic platforms were provided for rapid AST and minimum inhibitory concentration (MIC) determination.[15−24] These devices focus on reducing the assay time or increasing the assay throughput by utilizing high aspect ratio channels, droplets,[16,19,22] dielectrophoresis,[17,24] concentration gradient generators,[15,20] and centrifugal microfluidics.[18,21,23] Compared with traditional bulk incubation, the bacteria growing on-chip can reach their MIC value much faster,[25] allowing antimicrobial resistance analysis to be completed in as little as 2 h and reducing reagent and sample consumption.[26] By increasing the number of chambers, these devices can also provide the opportunity to analyze multiple antibiotics and multiple samples in parallel.

Unlike other microfluidic devices, centrifugal microfluidic technology does not require complex instruments, and it allows for the rapid acquisition of sufficient microbial cells for downstream AST and identification, avoiding the lengthy incubation process of traditional methods.[18,21,23] For example, Cho et al. developed a custom-made fidget spinner that could rapidly concentrate pathogens in 1 mL of undiluted urine by more than 100-fold for the on-device colorimetric detection of bacterial load and pathogen identification, which can be used for AST.[21] Xu et al. presented a centrifugation-based microfluidic concentrator for milliliter to picoliter bacteria suspension enrichment to achieve fast and real-time pathogen detection and AST within 3 h.[23] The above techniques allow easy measurement of the growth levels of broad-spectrum strains through a simple working principle. However, these microfluidic devices were mainly designed for purified, concentrated, viable microorganisms after subculture or urine samples with a simple composition. The lack of on-chip complex sample preparation processes still poses a significant challenge for their practical application.[27]

Herein, we introduced a bacteria separation integrated AST (BSI-AST) chip, which significantly shortened the turnaround time for positive blood cultures (PBCs). The integrated chip includes a bacteria separation chamber, multiple AST chambers, and connection channels. The separator gel preloaded in the bacteria separation chamber can rapidly separate bacteria from PBCs. Then, the bacteria suspension is distributed in downstream arrayed chambers preloaded with antibiotic solution using a quick vacuum-assisted aliquoting strategy. Through centrifugation of the integrated chip, bacteria cells from each chamber are completely enriched and collected at the tip of the AST chambers. As a result, significant growth inhibition can be observed after only a few hours of incubation. It could avoid the complicated and time-consuming solid-phase incubation process and realize rapid AST directly for the PBCs, which could save up to 2 days of clinical diagnostic time. We believe that this method will be very valuable in clinical application.

MATERIALS AND METHODS

Chemicals and Reagents. The chemicals and reagents are shown in the Supporting Information.

Preparation of PBCs. The Clinical and Laboratory Standards Institute (CLSI) standard strains (*Escherichia coli* ATCC 25922 and ATCC 35218) were both purchased from the American Type Culture Collection (ATCC; Manassas). Stock solutions were made using 25% glycerol (Sigma-Aldrich, MO, United States) and stored at −80 °C.

Standard CLSI strains *E. coli* ATCC 25922 and ATCC 35218 were inoculated onto LB agar plates and incubated overnight at 37 °C to grow into visible monoclonal clones. Bacterial isolates cultured overnight were diluted and then added to 5 mL of pig blood with an initial concentration of 100−200 CFU/mL. After that, the blood was inoculated into a resin aerobic blood bottle to simulate blood cultures, which were then incubated in an incubator until the blood culture bottles were positive. The fresh pig blood was purchased from Geran Biotechnology Co., Ltd. (Weifang, China).

Direct AST from Clinical Samples. Clinically positive blood culture bottles were provided by the Department of Clinical Laboratory, Qingdao University Affiliated Hospital (Qingdao). The seeded blood culture bottles were flagged as positive for microbial growth by a BACTEC FX automated incubation system (Becton Dickinson Company, NJ, United States) and appeared to be monomicrobial by Gram staining used in this study. For AST with the BSI-AST chip, the PBCs were directly performed on-chip AST without the subculture. To perform AST using the VITEK-2 Compact system (based on a microdilution broth method), the suspension from PBCs was inoculated on blood culture agar plates overnight at 37 °C to obtain a bacterial colony. The bacterial colonies were then diluted with 0.45% saline and adjusted to a density of 0.5 McFarland. Subsequently, 145 or 280 μL of bacterial solution was diluted to 3 mL and inoculated into VITEK cards. The VITEK cards were loaded into a VITEK-2 Compact automated reader-incubator for further analysis.

RESULTS AND DISCUSSION

Design and Fabrication of the BSI-AST Chip. The BSI-AST chip contains a bacteria separation chamber, multiple AST chambers, and connection channels. We fabricated two types of chips (BSI-AST chips I and II). BSI-AST chip I contains 5 AST chambers and is made of PDMS material for proof of concept. BSI-AST chip II contains 60 AST chambers and is packaged with double-sided tape and glass for clinical applications and high-throughput detection. The fabrication processes of the BSI-AST chips are depicted in the Supporting Information.

The structures of BSI-AST chips I and II are shown in Figure 1a,b, and the detailed dimensions of the main view of

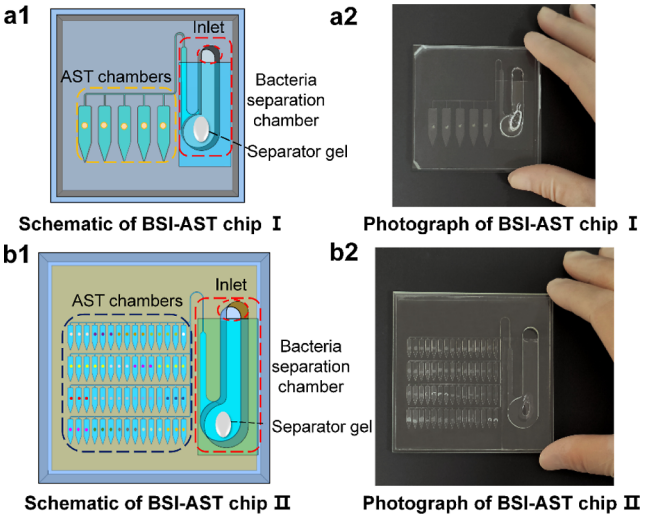

Figure 1. Schematic overview of the design and fabrication of the BSI-AST chip. (a1,a2) Schematic and photograph of BSI-AST chip I. (b1,b2) Schematic and photograph of BSI-AST chip II.

https://doi.org/10.1021/acs.analchem.3c02737
Anal. Chem. 2023, 95, 14375−14383

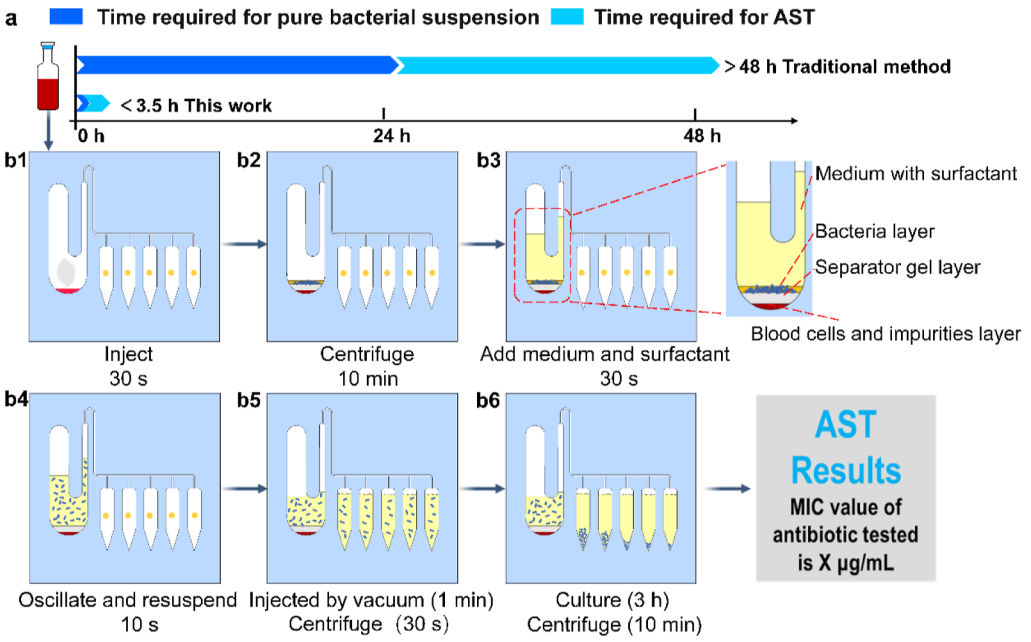

Figure 2. Workflow of rapid bacterial separation and AST from PBCs. (a) Conventional AST system requires three overnight culture steps: blood culture, subculture, and AST culture. The whole process takes >48 h, starting from PBCs. The BSI-AST chip can directly process PBCs without subculture. The whole process of AST from PBCs to report took <3.5 h. (b1−b6) The procedure of bacterial separation and AST from PBCs using the BSI-AST chip. Each step has a corresponding illustration.

both chips are shown in Figure S3. The bacteria separation chamber is U-shaped, with separator gel loaded at the U-shaped chamber bottom. The bacteria separation chamber and the AST chambers share an inlet, and the inlet is located at the top of the bacteria separation chamber. The AST chambers were connected to the bacteria separation chamber through multiple connection channels. To ensure that the bacteria separation chamber and AST chambers do not interfere with each other, we designed the size of the bacteria separation chamber according to the volume of the separator gel and sample, as well as the liquid volume of the AST chambers, to ensure that the sample does not enter the left microchannel until the bacterial separation in the PBCs is completed.

Workflow of the BSI-AST Chip. The traditional AST often requires three overnight culture steps: blood culture, subculture, and AST culture. The whole process takes over 48 h, starting from PBCs (Figure 2a). The workflow of the BSI-AST chip for rapid bacteria separation from PBCs and AST is shown in Figure 2(b1−b6). First, 25 μL of PBCs were injected directly into the bacteria separation chamber. The chip was fixed onto the 3D-printed chip holder and well protected with a sponge from breakage (Figure S4a−c). Then, the chip holder was put into a centrifuge (Allegra X-12 Beckman Coulter, USA), shown in Figure S4c, and centrifuged horizontally at 1500g for 10 min. The orientation of the centrifuge during centrifugation is always horizontally clockwise. Second, 500 μL of CAMHB was added to the bacteria separation chamber with 2‰ surfactant to prevent nonspecific adsorption on the AST chamber interface and mixed with the bacteria suspension on the top of the separator gel. Then, the chip was put into the vacuum device vertically (Figure S4d), and the vacuum degree was set at 150 mbar for 1 min. When the atmospheric pressure was restored, the separated bacteria suspension was distributed in downstream AST chambers through a quick vacuum-assisted aliquoting strategy. Since the vacuum degree was set to 150 mbar, there was still some air remaining at the bottom of the AST chambers. To completely dissolve the antibiotics in each chamber and ensure that the air bubbles at the bottom were located at the top of each AST chamber, the chip was centrifuged horizontally at 300g for 10 s again. Subsequently, the chip with the bacterial suspension was incubated vertically at 37 °C for 3 h. After incubation, the chip was centrifuged horizontally at 500g for 10 min. By centrifugation, nearly all of the bacteria cells were aggregated at the tip of the AST chambers. Since the material of the chip has good optical properties, the bacteria cells at the tip could be clearly imaged. The bacterial area was used to determine the antimicrobial susceptibility. The whole process of AST from PBCs to the resultant output took less than 3.5 h.

Principle of Bacteria Separation. The bacteria separation chamber of the integrated chip was loaded with a separator gel. The gel exhibits thixotropic properties, enabling it to flow during centrifugation. Separator gels are designed with a specific density that falls between those of the serum or plasma and the cells, thus determining the location of the interface. These characteristics make it an ideal material for separating two phases with different densities by centrifugation.[28] In PBCs, bacteria are mixed with a large number of blood cells, and the bacterial concentration ranges from 10^7 to 10^9 CFU/mL.[14] With reference to the relative sedimentation properties of blood components and bacteria,[29] the sedimentation velocities of the various blood components are different. Specifically, the sedimentation velocity of white blood cells (WBCs) is about 96 times faster than that of *E. coli*, and that of red blood cells (RBCs) is 30 times faster than that of *E. coli*. Therefore, the principles of sedimentation velocity may be used to separate bacteria. Under the action of centrifugal force, an appreciable fraction of bacteria and some platelets will collect on the separator gel surface after the formation of the gel plug and will not be able to penetrate.[29] Since platelets are produced through the proliferation and division of megakaryocytes in the bone marrow, the number of platelets does

https://doi.org/10.1021/acs.analchem.3c02737
Anal. Chem. 2023, 95, 14375−14383

not increase on its own in vitro. In addition, platelets are transparent and colorless, which means that any remaining platelets in the sample do not affect the microscopic imaging observations in the downstream AST chambers. Therefore, the principles of the thixotropy of the separator gel and the difference in sedimentation velocity between blood cells and bacteria may be used to separate bacteria from PBCs (Figure 3a).

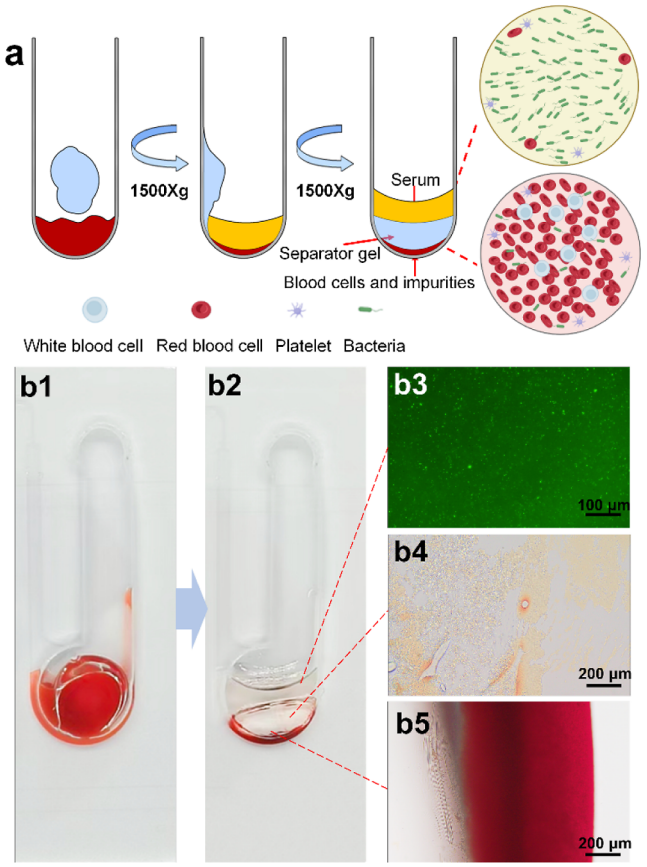

Figure 3. Principle of bacteria separation from PBCs with separator gel. (a) Thixotropic properties of separator gel and delamination of PBCs during centrifugation. (b1,b2) Photographs of the bacteria separation chamber. (b3) Bacteria layer. (b4) Separator gel layer. (b5) Blood cells and impurities layer.

To evaluate the effectiveness of bacteria separation from PBCs, a simulation test of GFP-labeled *E. coli* was performed on the integrated chip. We injected 200 μL of PBCs into the chip, centrifuged at 1500*g* for 10 min, and then imaged each part of the bacteria separation chamber after centrifugation. As shown in Figure 3(b1,b2), it could be seen that the separator gel became less viscous during centrifugation, which was adapted to the shape of the chip. The bacteria cells were separated to the upper layer of the separator gel, and blood cells were in the lower layer of the separator gel (Figures 3(b2−b5) and S5). It indicated that this on-chip separator gel strategy could rapidly obtain pure and high-concentration bacteria suspensions from PBCs.

Purity and Activity of Isolated Bacteria. To evaluate the recovery efficiency of bacteria cells and the removal efficiency of blood cells via the bacteria separation chamber from PBCs, we injected 500 μL of PBCs containing *E. coli* ATCC 25922 into the integrated chip and centrifuged at 1500*g* for 10 min. After centrifugation, the bacteria suspension on top of the gel was mixed well. The separated bacterial suspension and the spiked PBCs were serially diluted and plated to estimate the bacterial concentration (Figures 4(a1,a3), and S6). The bacterial recovery efficiency is the ratio of the bacterial concentration in the separated bacteria suspension and the concentration in the initial spiked PBCs, accounting for the dilution factor and sample volume (Figure S6). The RBC concentration was estimated by a hemocytometer in which the separated bacteria suspension was added directly to the hemocytometer, and spiked PBCs were first diluted 100 times and then added to the hemocytometer (Figure 4(a2,a4)). As shown in Figure 4b, the recovery efficiency of bacteria was about 40−61% (n = 3), while the removal efficiency of RBCs was around 99% (n = 3) from PBCs. It indicated that bacteria cells could be rapidly separated from undiluted PBCs, and the majority of RBCs were removed by the integrated chip.

To ensure the activity of the target pathogenic bacteria after separation, we used Raman microspectroscopy coupled with D_2O labeling to characterize the metabolic activity of bacteria. The cell metabolic activity was expressed by the C−D (carbon−deuterium vibration) ratio of Raman spectra,[30] which was calculated by dividing the C−D peak area at Raman shifts 2040−2300 cm^{-1} by the sum of the C−H peak area at Raman shifts 2800−3100 cm^{-1} and the C−D peak area. For *E. coli*, D_2O labeling is usually completed after incubation at 37 °C for 2.5 h.[31] To evaluate the effect of the separator gel and residual blood culture components on the metabolic activity of the bacteria. Here, the pure bacterial suspension cultured overnight was used as the control group, and the bacterial suspension separated from PBCs was used as the experimental group. The D_2O culture medium was added to both groups to a final concentration of D_2O of 50%. After 2.5 h of incubation, the samples were centrifuged and deposited on glass slides for Raman detection (532 nm laser), and the Raman spectra of the two groups were normalized and averaged separately to calculate mean C−D ratios. The results are shown in Figure 4c,d. There was no significant difference in the Raman spectrum or C−D ratio (0.033 vs 0.030) between the two groups. It indicated that the separator gel and residual blood culture components had no significant effect on the metabolic activity of the bacteria.

Consistency of the Filled Volume in AST Chambers. Another important point of the BSI-AST chip is the consistency of the filled volume in the AST chambers of the BSI-AST chip. Figure 5(a1−a3) demonstrates the filling process with the amaranth red liquid. First, 500 μL of amaranth red liquid was added into the bacteria separation chamber (Figure 5(a1)). After 1 min of vacuum at 150 mbar, when atmospheric pressure was restored, the liquid in the bacteria separation chamber would be rapidly and uniformly dispensed into the AST chambers driven by negative pressure (Figure 5(a2)). In order to isolate the liquid in each AST chamber, the chip was transiently centrifuged at 300*g* for 10 s again. At this time, the liquid in the main channel and the branch channel also entered the AST chambers (Figure 5(a3)), but the increase of liquid volume in each AST chamber was not obvious due to the short spin time. Figure 5b shows the percentage of the liquid-filled area in the AST chambers. The results of the one-way ANOVA (analysis of variance) showed that the statistical value of the data for the five chambers was P-value 0.122 > 0.05, indicating that there was no significant

https://doi.org/10.1021/acs.analchem.3c02737
Anal. Chem. 2023, 95, 14375−14383

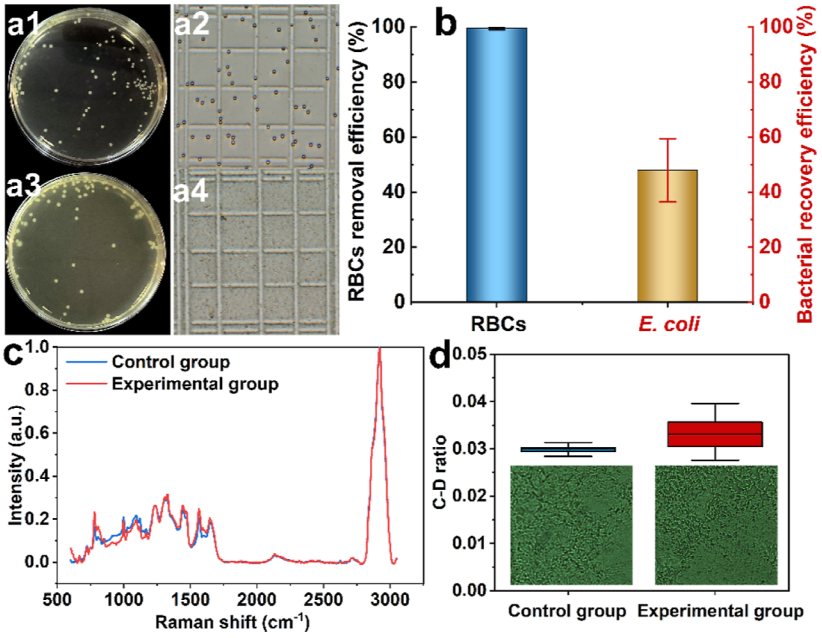

Figure 4. Purity and activity of bacteria isolated based on the BSI-AST chip. (a1,a3) The separated bacteria suspension and the spiked PBCs were serially diluted and plated to estimate the bacterial concentration. (a2,a4) The RBC concentration was estimated by a hemocytometer. The separated bacteria suspension was added directly to the hemocytometer, and spiked PBCs were first diluted 100 times and then added to the hemocytometer. (b) RBC removal efficiency and bacterial recovery efficiency. (c) Raman spectra of comparison of the experimental group and control group after D_2O feeding. (d) C−D ratios of the experimental group and control group after D_2O feeding.

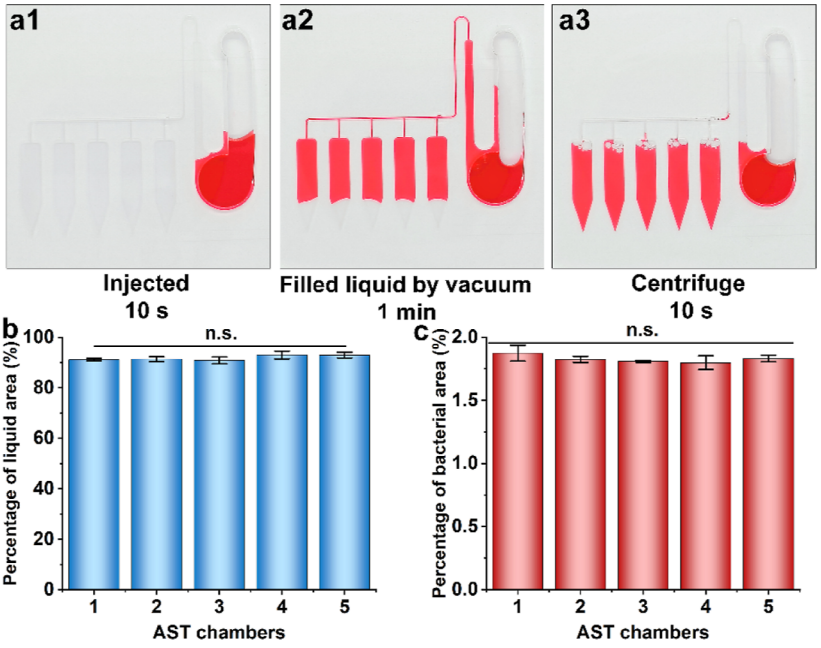

Figure 5. Overview and characteristics of the sample filling principle with the BSI-AST chip. (a1−a3) Red liquid filling process of the AST chambers. (b) Consistency of the filled liquid inside the AST chambers with three parallel experiments. (c) Consistency of bacterial growth inside the AST chambers after centrifugation with three parallel experiments.

difference in the filled liquid volume of the AST chambers. In addition, we followed the above procedure to incubate the bacteria suspension extracted from PBCs in the AST chambers without antibiotics for 3 h and then centrifuged to calculate the percentage of the bacterial area at the tip of the AST chambers (Figure S7). Figure 5c shows the statistical value of the data from the five chambers with a *P*-value of 0.271 > 0.05. It further proved that there was no significant difference in the filled volume of the bacteria suspension in the AST chambers. The above results demonstrated that the integrated chip could realize sensitivity testing of multiple antibiotics simultaneously.

Rapid AST from the Spiked PBCs. To validate the accuracy of the BSI-AST chip, we performed direct AST using spiked samples of two standard CLSI strains (*E. coli* ATCC 25922 and *E. coli* ATCC 35218) in blood culture bottles containing fresh pig blood. After AST culture, the integrated chip was placed directly under the microscope to observe the morphological changes of the bacteria and assess their

https://doi.org/10.1021/acs.analchem.3c02737
Anal. Chem. 2023, 95, 14375−14383

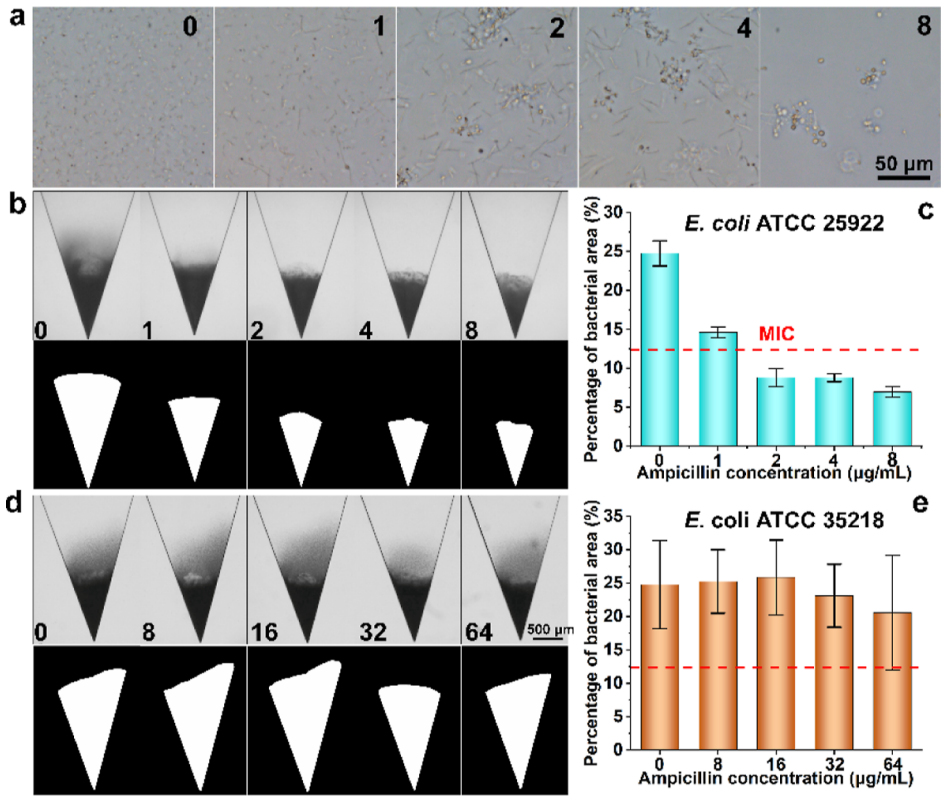

Figure 6. AST results for the spiked PBCs of standard strains in different concentrations of ampicillin based on the BSI-AST chip. Images with 4× objective were taken after 3 h of incubation after centrifuge and processed with ImageJ into binary format to enhance the contrast. (a) Morphological changes of the sensitive ATCC 25922 strains at different concentrations of ampicillin. (b) Sensitive ATCC 25922 strains at different concentrations of ampicillin. (c) Percentage of bacterial area of ATCC 25922 strains from processed images of three groups after 3 h incubation. (d) Resistant ATCC 35218 strains in different concentrations of ampicillin. (e) Percentage of bacterial area of ATCC 35218 strains from processed images of three groups after 3 h of incubation.

susceptibility to antibiotics. For the ATCC 25922 group (Figure 6a), at 1 μg/mL of ampicillin, some bacterial cells started to become filamentous. When the concentration reached 2 μg/mL, almost all bacterial growth was inhibited. At a higher concentration of 8 μg/mL, most of the bacteria rapidly lysed before forming filamentous cells.

To further illustrate the growth difference in AST chambers, the BSI-AST chip was centrifuged at 500*g* for 10 min after AST culture, and nearly all the bacteria cells were aggregated at the tip of the AST chambers (Figure 6b). Here, all of the images were processed with ImageJ software (Figure 6b–d). Briefly, the images were converted to 8 bit format. Then the background of the channel in each image was distinguished from the area occupied by bacterial cells by adjusting the threshold function with a threshold range of 180–255, after which we subtracted the excess edges, and finally, the percentage of the bacterial area to the whole image was calculated by the Analyze Particles function. The MIC can be determined by the growth differences in different concentrations of antibiotics. As shown in Figure 6b,c, for the ATCC 25922 group, a significant inhibition was observed on the growth of bacteria cells at 2 μg/mL ampicillin. The calculated percentage of bacterial area dropped from 24.7 to 8.8%. The percentage of bacterial area decreased to 35.6% (<50%) of the control. When the ampicillin concentration was increased to 8 μg/mL, percentage of bacterial area dropped to 7.0%. The percentage no longer decreased significantly with increasing concentrations. It indicated that all cells were killed in this concentration range. Therefore, the MIC of ATCC 25922 for ampicillin was 2 μg/mL, which was consistent with the sensitivity observed by bacterial morphology. Thus, a threshold where the bacterial area percentage was less than 50% of the control groups was given here for the MIC determination. For the ATCC 35218 group (Figure 6d,e), there was no obvious decrease in the percentage of bacterial area (25.8–20.6%) compared to the control group in 0–64 μg/mL ampicillin. It indicated that no obvious growth inhibition had occurred. In summary, the MIC of ATCC 25922 for ampicillin was 2 μg/mL and ATCC 35218 for ampicillin was >64 μg/mL. The MIC values based on the BSI-AST chip were within the CLSI quality control (QC) ranges.

The blood bacterial resistant investigation collaborative system (BRICS) report surveillance results from 2014 to 2019 show that the main pathogens of bloodstream infection in China are Gram-negative bacteria, in which *E. coli* and *Klebsiella pneumoniae* were the main BSI pathogens during the surveillance period.[32] Therefore, we have used the BSI-AST chip to design a special AST card for Enterobacteriaceae bacteria, which contains 18 types of antibiotics approved by the Food and Drug Administration (FDA). We performed direct AST using spiked samples of two standard CLSI strains (*E. coli* ATCC 25922 and *E. coli* ATCC 35218) in blood culture bottles containing fresh blood. Figure S8 shows the AST results of *E. coli* ATCC 25922 against 18 antibiotics and *E. coli* ATCC 35218 against three antibiotics, respectively. Since *E. coli* ATCC 35218 was used for quality control of β-

https://doi.org/10.1021/acs.analchem.3c02737
Anal. Chem. 2023, 95, 14375–14383

lactam/β-lactam inhibitors, we tested only three drugs (ampicillin, ampicillin sulbactam, and amoxicillin clavulanate).

The MICs determined using the preestablished threshold were consistent with the results obtained from the CLSI protocol (Table S1). These results indicated that the BSI-AST chip was validated as a direct and rapid AST method for PBCs. The BSI-AST chip could greatly shorten and simplify the tedious and labor-intensive procedures for current standard AST methods.

Direct and Rapid AST from Clinical PBCs. To further validate the applicability of the BSI-AST chip, we tested the performance of the BSI-AST chip in actual clinical PBC samples, which included *E. coli* (three PBCs) and *K. pneumoniae* (one PBCs). After MALDI TOF-based species identification, we performed direct AST and determined MIC values using the BSI-AST chip, and another copy of the sample was tested by the clinical laboratory staff using the VITEK-2 Compact system (based on the microdilution broth method) and the K−B method (disk diffusion method). First, the integrated chip could realize the isolation of target pathogenic bacteria in clinical PBCs (Figure S9). The on-chip AST results closely matched those reported by the automated system-based standard methods. It showed an overall 93.3% (Table S2 and Figures S10−S13) categorical agreement with clinical results. At the same time, the on-chip AST results were yielded within 3.5 h after blood culture positivity, while clinical standard methods take over 48 h from PBCs to result readout. Moreover, the accuracy of the on-chip AST results could be further improved. For instance, in clinical PBC sample no. 4, the bacterial cell division was blocked, resulting in the formation of filamentous bodies under the environment of aztreonam (4−16 μg/mL). Based on morphological observation and clinical experience, clinical PBC sample no. 4 is sensitive to aztreonam, but the result was judged as resistant based on the calculation of bacterial area (Figure S14). This was mainly due to the short incubation time for AST. Therefore, if a quick determination is required, it is best to consider additional parameters beyond the bacterial area in the judgment, which will further improve the accuracy of the results.

In addition, this article primarily focuses on Enterobacteriaceae bacteria as an example for methodological validation. However, the potential threat of drug resistance caused by Gram-positive bacteria should not be overlooked. We evaluated the effectiveness of Gram-positive bacteria separation from PBCs using the integrated chip, using *Staphylococcus aureus* as an example. The results indicated that this method successfully isolated *S. aureus* from PBCs, resulting in a high-purity suspension (Figure S15). However, there was a significant difference in the concentrations of the separated bacterial suspension between *S. aureus* and *E. coli*. Hence, the integrated chip-based processing workflow mentioned in this paper is not suitable for Gram-positive bacteria. Therefore, we need to reconsider the entire operating workflow for Gram-positive bacteria to meet the bacterial concentration requirements for AST. This research work will be systematically carried out in the future. Finally, compared to previous studies, the BSI-AST chip has the advantages of integration, convenience, and rapid detection. The bacteria separation from PBCs and AST was achieved on the BSI-AST chip, which greatly simplifies the operation and shortens the turnaround time. More importantly, the chip design establishes a bridge between macroscopic sample preprocessing and microscopic rapid detection. The integrated chip will be a promising tool for the direct detection of other complex body fluid samples and is expected to be coupled with other bioassays, such as Raman microspectroscopy identification.[33]

CONCLUSIONS

In this work, an integrated chip was developed for direct AST from the PBCs without subculture. Separator gel was added to the chip for the first time and achieved rapid extraction and enrichment of bacteria from PBCs. In combination with centrifugal microfluidic enrichment technology, AST results could be obtained in less than 3.5 h from PBCs. We demonstrated the multiplexing analysis capability of the integrated chip by introducing antibiotic drying and array parallelization. As a proof of concept, the susceptibility patterns of PBCs containing *E. coli* against 18 antibiotics were determined. Moreover, the BSI-AST chip was also used to perform direct AST from clinical PBCs, and the on-chip AST results highly matched clinical results with 93.3% categorical agreement. Reliable AST results would be available within 3.5 h from PBCs, which would help clinicians promptly confirm or streamline effective antibiotic therapy in patients with BSIs.

Our aim for the future is to configure the BSI-AST chip, centrifuge, and vacuum device used into a compact automated system that enables sample input and result output and requires minimal user intervention. Finally, we will perform a large-scale side-by-side comparison of the performance of the BSI-AST chip device with the current gold standard method to assess the clinical statistical significance of our method.

ASSOCIATED CONTENT

Supporting Information

The Supporting Information is available free of charge at https://pubs.acs.org/doi/10.1021/acs.analchem.3c02737.

> Chemicals and reagents; fabrication of the BSI-AST chip; schematic and photograph of the chip holder and instrument; dimensions of the main view of the BSI-AST chips; removal of blood cells and isolation of bacteria from spiked PBCs and clinical PBCs via the BSI-AST chip; image of bacteria incubated in an AST chamber for 3 h and centrifuged; quantification of *E. coli* in the original spiked PBCs and bacteria suspensions separated from the spiked PBCs; AST results for the spiked PBCs of standard strains based on the BSI-AST chip; AST results reported by the BSI-AST chip for clinical PBCs; comparison of MIC values from the BSI-AST chip with spiked PBCs and standard reference values from CLSI; comparison of AST results for clinical PBCs reported by the BSI-AST chip and the clinical standard methods; and comparison of the BSI-AST chip with previous methods (PDF)

AUTHOR INFORMATION

Corresponding Author

Yongqiang Cheng − *School of Environmental Science and Engineering, Institute of Eco-Environmental Forensics, Shandong University (Qingdao), Qingdao, Shandong 266237, China;* orcid.org/0000-0002-4539-3448; Phone: +86-15092127156; Email: chengyongqiang@sdu.edu.cn

https://doi.org/10.1021/acs.analchem.3c02737
Anal. Chem. 2023, 95, 14375−14383

Authors

Meijia Zhu − *School of Environmental Science and Engineering, Institute of Eco-Environmental Forensics, Shandong University (Qingdao), Qingdao, Shandong 266237, China*

Teng Xu − *Single-Cell Center, CAS Key Laboratory of Biofuels, Shandong Key Laboratory of Energy Genetics, Shandong Energy Institute, Qingdao Institute of Bioenergy and Bioprocess Technology, Chinese Academy of Sciences, Qingdao, Shandong 266101, China; University of Chinese Academy of Sciences, Beijing 100049, China*

Bo Ma − *Single-Cell Center, CAS Key Laboratory of Biofuels, Shandong Key Laboratory of Energy Genetics, Shandong Energy Institute, Qingdao Institute of Bioenergy and Bioprocess Technology, Chinese Academy of Sciences, Qingdao, Shandong 266101, China; University of Chinese Academy of Sciences, Beijing 100049, China;* orcid.org/0000-0002-8501-772X

Jian Xu − *Single-Cell Center, CAS Key Laboratory of Biofuels, Shandong Key Laboratory of Energy Genetics, Shandong Energy Institute, Qingdao Institute of Bioenergy and Bioprocess Technology, Chinese Academy of Sciences, Qingdao, Shandong 266101, China; University of Chinese Academy of Sciences, Beijing 100049, China;* orcid.org/0000-0002-0548-8477

Zhidian Diao − *Single-Cell Center, CAS Key Laboratory of Biofuels, Shandong Key Laboratory of Energy Genetics, Shandong Energy Institute, Qingdao Institute of Bioenergy and Bioprocess Technology, Chinese Academy of Sciences, Qingdao, Shandong 266101, China; University of Chinese Academy of Sciences, Beijing 100049, China*

Fei Wu − *Single-Cell Center, CAS Key Laboratory of Biofuels, Shandong Key Laboratory of Energy Genetics, Shandong Energy Institute, Qingdao Institute of Bioenergy and Bioprocess Technology, Chinese Academy of Sciences, Qingdao, Shandong 266101, China*

Jing Dai − *Single-Cell Center, CAS Key Laboratory of Biofuels, Shandong Key Laboratory of Energy Genetics, Shandong Energy Institute, Qingdao Institute of Bioenergy and Bioprocess Technology, Chinese Academy of Sciences, Qingdao, Shandong 266101, China*

Xiao Han − *Single-Cell Center, CAS Key Laboratory of Biofuels, Shandong Key Laboratory of Energy Genetics, Shandong Energy Institute, Qingdao Institute of Bioenergy and Bioprocess Technology, Chinese Academy of Sciences, Qingdao, Shandong 266101, China; School of Chemistry and Chemical Engineering, University of Jinan, Jinan, Shandong 250024, China*

Pengfei Zhu − *Single-Cell Center, CAS Key Laboratory of Biofuels, Shandong Key Laboratory of Energy Genetics, Shandong Energy Institute, Qingdao Institute of Bioenergy and Bioprocess Technology, Chinese Academy of Sciences, Qingdao, Shandong 266101, China; Qingdao Single Cell Biotechnology Company Limited, Qingdao, Shandong 266000, China*

Chao Pang − *Single-Cell Center, CAS Key Laboratory of Biofuels, Shandong Key Laboratory of Energy Genetics, Shandong Energy Institute, Qingdao Institute of Bioenergy and Bioprocess Technology, Chinese Academy of Sciences, Qingdao, Shandong 266101, China*

Jing Li − *Department of Clinical Laboratory, The Affiliated Hospital of Qingdao University, Qingdao, Shandong 266003, China*

Hongwei Wang − *Department of Clinical Laboratory, The Affiliated Hospital of Qingdao University, Qingdao, Shandong 266003, China*

Ranran Xu − *School of Environmental Science and Engineering, Institute of Eco-Environmental Forensics, Shandong University (Qingdao), Qingdao, Shandong 266237, China*

Xiaotong Li − *School of Environmental Science and Engineering, Institute of Eco-Environmental Forensics, Shandong University (Qingdao), Qingdao, Shandong 266237, China*

Complete contact information is available at: https://pubs.acs.org/10.1021/acs.analchem.3c02737

Notes

Protocols of this study were reviewed and approved by the Ethics Committee of the Qingdao Institute of BioEnergy and Bioprocess Technology, Chinese Academy of Sciences. As all bacterial strains were from residual samples used in clinical diagnosis or strains from their subcultures, the criteria for exemption were met.

The authors declare no competing financial interest.

■ ACKNOWLEDGMENTS

Financial supports from the Natural Science Foundation of Shandong Province (no. ZR2021MB082), the Fundamental Research Funds of Shandong University (no. 2020GN022), the Natural Science Foundation of China (no. 21207080), and the National Key Technology R&D Program of the Ministry of Science and Technology (no. 2012BAF14B04) are gratefully acknowledged.

■ REFERENCES

(1) Costa, S. P.; Dias, N. M.; Melo, L. D. R.; Azeredo, J.; Santos, S. B.; Carvalho, C. M. *Sci. Rep.* **2020**, *10* (1), 6260.

(2) Rhee, C.; Dantes, R.; Epstein, L.; Murphy, D. J.; Seymour, C. W.; Iwashyna, T. J.; Kadri, S. S.; Angus, D. C.; Danner, R. L.; Fiore, A. E.; Jernigan, J. A.; Martin, G. S.; Septimus, E.; Warren, D. K.; Karcz, A.; Chan, C.; Menchaca, J. T.; Wang, R.; Gruber, S.; Klompas, M.; Program, C. D. C. P. E. *J. Am. Med. Assoc.* **2017**, *318* (13), 1241−1249.

(3) Brown, R. M.; Wang, L.; Coston, T. D.; Krishnan, N. I.; Casey, J. D.; Wanderer, J. P.; Ehrenfeld, J. M.; Byrne, D. W.; Stollings, J. L.; Siew, E. D.; Bernard, G. R.; Self, W. H.; Rice, T. W.; Semler, M. W. *Am. J. Respir. Crit. Care Med.* **2019**, *200* (12), 1487−1495.

(4) Charles, P. E.; Dalle, F.; Aube, H.; Doise, J. M.; Quenot, J. P.; Aho, L. S.; Chavanet, P.; Blettery, B. *Intensive Care Med.* **2005**, *31* (3), 393−400.

(5) Lagu, T.; Rothberg, M. B.; Shieh, M. S.; Pekow, P. S.; Steingrub, J. S.; Lindenauer, P. K. *J. Crit. Care* **2012**, *27* (4), 414.e1−414.e9.

(6) Arnold, H. M.; Micek, S. T.; Skrupky, L. P.; Kollef, M. H. *Semin. Respir. Crit. Care Med.* **2011**, *32* (02), 215−227.

(7) Laxminarayan, R.; Duse, A.; Wattal, C.; Zaidi, A. K.; Wertheim, H. F.; Sumpradit, N.; Vlieghe, E.; Hara, G. L.; Gould, I. M.; Goossens, H.; Greko, C.; So, A. D.; Bigdeli, M.; Tomson, G.; Woodhouse, W.; Ombaka, E.; Peralta, A. Q.; Qamar, F. N.; Mir, F.; Kariuki, S.; Bhutta, Z. A.; Coates, A.; Bergstrom, R.; Wright, G. D.; Brown, E. D.; Cars, O. *Lancet Infect. Dis.* **2013**, *13* (12), 1057−1098.

(8) Leuthner, K. D.; Doern, G. V. *J. Clin. Microbiol.* **2013**, *51* (12), 3916−3920.

(9) Kumar, A.; Roberts, D.; Wood, K. E.; Light, B.; Parrillo, J. E.; Sharma, S.; Suppes, R.; Feinstein, D.; Zanotti, S.; Taiberg, L.; Gurka, D.; Kumar, A.; Cheang, M. *Crit. Care Med.* **2006**, *34* (6), 1589−1596.

(10) Filbrun, A. B.; Richardson, J. C.; Khanal, P. C.; Tzeng, Y. L.; Dickson, R. M. *Cytometry, Part A* **2022**, *101* (7), 564−576.

(11) Carrigan, S. D.; Scott, G.; Tabrizian, M. *Clin. Chem.* **2004**, *50* (8), 1301−1314.
(12) Jorgensen, J. H.; Ferraro, M. J. *Clin. Infect. Dis.* **2009**, *49* (11), 1749−1755.
(13) Li, Y.; Yan, X.; Feng, X.; Wang, J.; Du, W.; Wang, Y.; Chen, P.; Xiong, L.; Liu, B. F. *Anal. Chem.* **2014**, *86* (21), 10653−10659.
(14) Choi, J.; Jeong, H. Y.; Lee, G. Y.; Han, S.; Han, S.; Jin, B.; Lim, T.; Kim, S.; Kim, D. Y.; Kim, H. C.; Kim, E. C.; Song, S. H.; Kim, T. S.; Kwon, S. *Sci. Rep.* **2017**, *7* (1), 1148.
(15) Azizi, M.; Davaji, B.; Nguyen, A. V.; Zhang, S.; Dogan, B.; Simpson, K. W.; Abbaspourrad, A. *ACS Sens.* **2021**, *6* (4), 1560−1571.
(16) Boedicker, J. Q.; Li, L.; Kline, T. R.; Ismagilov, R. F. *Lab Chip* **2008**, *8* (8), 1265−1272.
(17) Chen, K. H.; Lee, S. H.; Kok, L. C.; Ishdorj, T. O.; Chang, H. Y.; Tseng, F. G. *Biosens. Bioelectron.* **2022**, *197*, 113740.
(18) Hwang, S.; Choi, J. *Lab Chip* **2023**, *23* (2), 229−238.
(19) Kaushik, A. M.; Hsieh, K.; Chen, L.; Shin, D. J.; Liao, J. C.; Wang, T. H. *Biosens. Bioelectron.* **2017**, *97*, 260−266.
(20) Kim, K. P.; Kim, Y. G.; Choi, C. H.; Kim, H. E.; Lee, S. H.; Chang, W. S.; Lee, C. S. *Lab Chip* **2010**, *10* (23), 3296−3299.
(21) Michael, I.; Kim, D.; Gulenko, O.; Kumar, S.; Kumar, S.; Clara, J.; Ki, D. Y.; Park, J.; Jeong, H. Y.; Kim, T. S.; Kwon, S.; Cho, Y.-K. *Nat. Biomed. Eng.* **2020**, *4* (6), 591−600.
(22) Scheler, O.; Pacocha, N.; Debski, P. R.; Ruszczak, A.; Kaminski, T. S.; Garstecki, P. *Lab Chip* **2017**, *17* (11), 1980−1987.
(23) Xu, T.; Han, X.; Zhu, P.; Dai, J.; Liu, M.; Liu, Y.; Xu, J.; Ma, B. *Sens. Actuators, B* **2021**, *343*, 130117.
(24) Yi, Q.; Cai, D.; Xiao, M.; Nie, M.; Cui, Q.; Cheng, J.; Li, C.; Feng, J.; Urban, G.; Xu, Y. C.; Lan, Y.; Du, W. *Biosens. Bioelectron.* **2019**, *135*, 200−207.
(25) Cira, N. J.; Ho, J. Y.; Dueck, M. E.; Weibel, D. B. *Lab Chip* **2012**, *12* (6), 1052−1059.
(26) Chen, C. H.; Lu, Y.; Sin, M. L.; Mach, K. E.; Zhang, D. D.; Gau, V.; Liao, J. C.; Wong, P. K. *Anal. Chem.* **2010**, *82* (3), 1012−1019.
(27) Dong, T.; Zhao, X. *Anal. Chem.* **2015**, *87* (4), 2410−2418.
(28) Lin, F.-C.; Cohen, R.; Losada, R.; Bush, V. *Lab. Med.* **2001**, *32* (10), 588−594.
(29) Pitt, W. G.; Alizadeh, M.; Husseini, G. A.; McClellan, D. S.; Buchanan, C. M.; Bledsoe, C. G.; Robison, R. A.; Blanco, R.; Roeder, B. L.; Melville, M.; Hunter, A. K. *Biotechnol. Prog.* **2016**, *32* (4), 823−839.
(30) Tao, Y.; Wang, Y.; Huang, S.; Zhu, P.; Huang, W. E.; Ling, J.; Xu, J. *Anal. Chem.* **2017**, *89* (7), 4108−4115.
(31) Yang, K.; Li, H. Z.; Zhu, X.; Su, J. Q.; Ren, B.; Zhu, Y. G.; Cui, L. *Anal. Chem.* **2019**, *91* (9), 6296−6303.
(32) Chen, Y.; Ji, J.; Ying, C.; Liu, Z.; Yang, Q.; Kong, H.; Xiao, Y.; Ding, H.; Liu, Y.; Mao, H.; Blood Bacterial Resistant Investigation Collaborative System Study Group. *Antimicrob. Resist. Infect. Control* **2022**, *11* (1), 17.
(33) Lorenz, B.; Rosch, P.; Popp, J. *Anal. Bioanal. Chem.* **2019**, *411* (21), 5445−5454.

https://doi.org/10.1021/acs.analchem.3c02737
Anal. Chem. 2023, 95, 14375−14383